

Ordered-defect model for Si(001)-(2×8)

Tetsuya Aruga* and Yoshitada Murata

The Institute for Solid State Physics, The University of Tokyo, 7-22-1 Roppongi, Minato-ku, Tokyo 106, Japan

(Received 5 December 1985; revised manuscript received 19 May 1986)

The atomic arrangement of the Si(001)-(2×8) surface, which is obtained by annealing at high temperatures, is discussed. Both the analysis of strong features in low-energy electron diffraction patterns and considerations about the surface strain energy favor the ordered missing-dimer defect model. The role of a trace of nickel impurity, which has been reported to stabilize the (2×8) structure, is also discussed.

Exhaustive investigations in this decade on the atomic structure of the Si(001) surface have found an almost universal agreement that the adjacent atoms in the top-most layer form a dimer by dangling bond pairing. Chadi¹ as well as Yin and Cohen² suggested by theoretical considerations that the buckling of dimers leads to a more stable structure. Recently, Tabata, Aruga, and Murata³ have shown by low-energy electron diffraction (LEED) that a transition from a low-temperature $c(4\times 2)$ phase to a high-temperature (2×1) phase occurs on Si(001) and that the basic atomic arrangement in the (2×1) unit mesh is conserved during the transition. This behavior was most naturally explained with the buckled-dimer model that the ground state is antiferromagnetic ordering, $c(4\times 2)$, of the buckled dimers and the orientation of buckled dimers is disordered above the critical temperature, $T_c = 200$ K. These results were in fruitful agreement with a renormalization-group calculation by Ihm *et al.*⁴ and a Monte Carlo simulation by Saxena *et al.*⁵

Muller *et al.*⁶ reported, however, that a *clean* Si(001) surface shows a (2×8) reconstruction after quenching from high temperature. On the other hand, McRae, Malic, and Kapilow⁷ and Ichinokawa *et al.*⁸ have found that a trace amount of Ni contamination leads to the (2×8) reconstruction. The reported LEED patterns from the “clean” and “Ni-contaminated” surfaces are, however, very similar to each other.

In the meantime, it is hard to conclude whether the (2×8) reconstruction can be stabilized only by Ni contamination or also by other factors. However, we should notice that, even for the apparently Ni-contaminated surface, it is very unlikely that the (2×8) periodicity is achieved by Ni atoms only, since the Ni concentration is reported to be below a few atomic percent.⁸ In this paper we report an analysis of the (2×8) LEED patterns and propose a structure model for the (2×8) reconstructed Si(001) surface. The model is based on the missing-dimer defect model proposed by Pandey⁹ and can elucidate the pronounced features of the (2×8) LEED patterns. Subsequently, the possible mechanisms of the formation of the (2×8) structure are presented with much attention paid to the role of a trace Ni.

Figure 1(a) shows a typical LEED pattern from another structure of the Si(001) surface, the (2×8) structure. This

was achieved by annealing at high temperature (1400–1600 K) and a rather rapid cooldown at a rate of several 10 K/sec. Any contamination, especially Ni or Cu, was not detected by Auger electron spectroscopy recorded by using a four-grid LEED optics. We have not strictly established the annealing and/or cooling condition for the formation of the (2×8) structure. It seems that the quenching from high temperature is not necessarily required for the (2×8) structure in contradiction to the suggestion by Muller *et al.*⁶ Prolonged annealing at lower temperatures (1200–1300 K) and slow cooldown sometimes gave a small portion of the (2×8) domains coexisting with the (2×1) structure. This implies the possibility of contamination by Ni during the annealing. We, however, sometimes observed a part of the sample surface exhibiting a clear (2×8) pattern, while the rest of the surface exhibiting (2×1) . This seems unlikely for the Ni-contaminated surface, since Ni atoms easily migrate and cover whole the sample surface when the sample is annealed.⁸ This fact may imply that some factors other than the Ni contamination, such as strain due to sample holding, can also stabilize the (2×8) structure when coupled with excess annealing.

LEED patterns from the (2×8) structure at different incident electron energies have common pronounced features. The intensity of the eighth-order spots was averaged over the LEED patterns at many different energies and is schematically illustrated in Fig. 1(b). Important features are as follows: (1) Among possible eighth-order spots, those neighboring fundamental spots [i.e., the spots of indices of $(n \pm \frac{1}{8}, k)$, where n is an integer and k an integer or a half-integer] are the most intense; (2) the spots of indices of $(n \pm \frac{3}{8}, k)$, $(n \pm \frac{4}{8}, k)$, and $(n \pm \frac{5}{8}, k)$ are almost always absent; (3) the spots of indices of $(n - \frac{1}{8}, k)$ and $(n - \frac{2}{8}, k)$ are more intense than those of indices of $(n + \frac{1}{8}, k)$ and $(n + \frac{2}{8}, k)$, respectively. This pattern is explained as that the “8” periodicity along the [10] direction is strongly modulated by a periodicity indicated by \mathbf{Q} , a magnitude of which is slightly shorter than that of the (10) reciprocal lattice vector. This suggests that the basic repeating unit along the [10] direction is a little longer than the (2×1) structure. These strong features, independent of incident electron energy or incidence an-

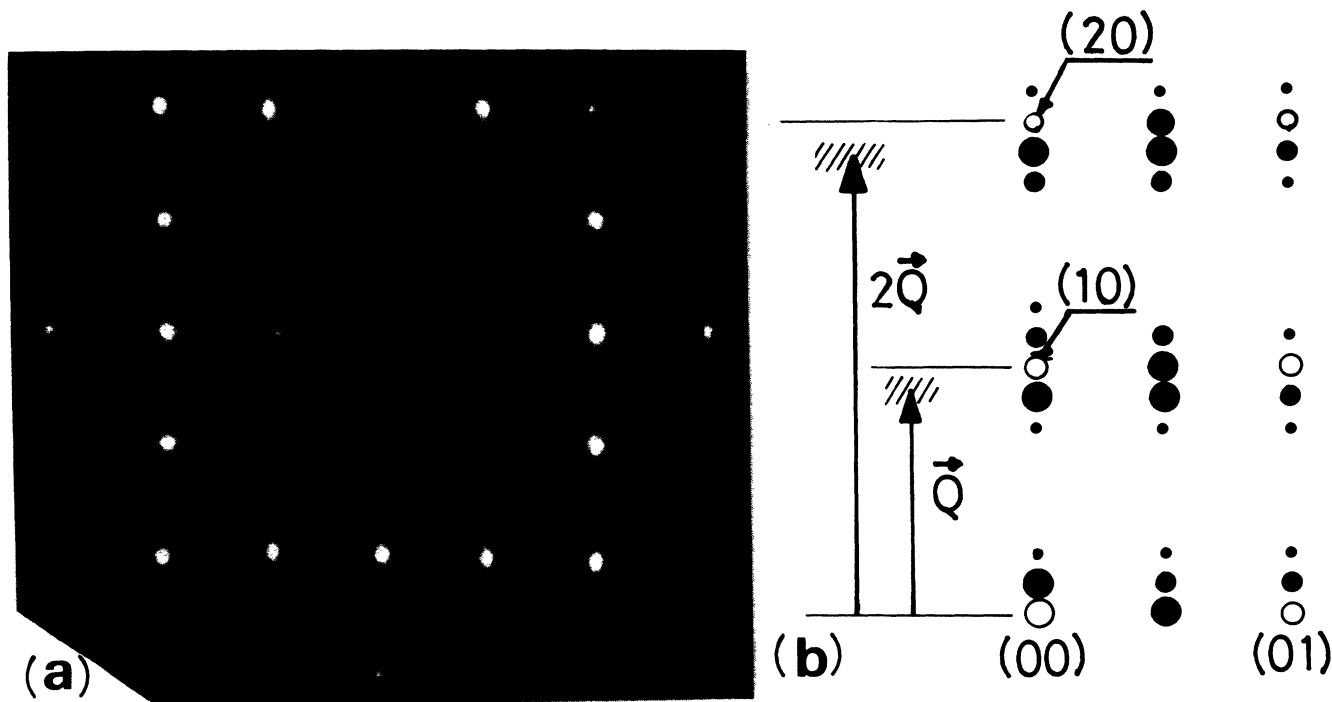


FIG. 1. (a) Typical LEED pattern of normal incidence from the two-domain Si(001)-(2×8) surface. Primary electron energy is 47 eV. (b) Averaged LEED pattern. Only the contribution from one of the two orthogonal domains is shown for the sake of simplicity.

gle, should dominantly have a kinematical origin. Any structure model for the (2×8) surface should, therefore, fulfill criteria as follows: First, because of the above-mentioned features (1) and (2), the local structure of the (2×8) surface is in gross similar to that of the (2×1) surface. This was also suggested by a strong similarity of intensity-versus-voltage (I - V) profiles of the (2×1) and (2×8) surfaces⁶ and implies that the dimer structure is mostly conserved in the (2×8) surface with weak 8-periods modulation along the direction of dimer rows. Secondly, because of the feature (3), spacing between adjacent atoms along the dimer row is slightly elongated as compared with the ideal (2×1) surface.

In order to elucidate the LEED patterns, we introduce an idea of missing-dimer defect which was first proposed by Pandey.⁹ He suggested that an atomic-scale defect as shown in Fig. 2(a) can reduce the number of dangling

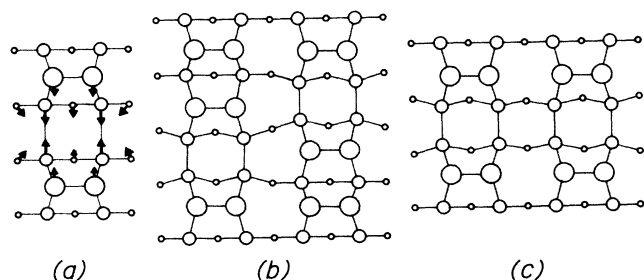


FIG. 2. Top view of the Si(001) surface with (a) a single defect, (b) a type-I pair of defects, (c) a type-II pair of defects. Large, medium, and small circles represent topmost-, second-, and third-layer atoms, respectively.

bonds and increase π bonding in adjacent dimer bonds. Tromp, Hamers, and Demuth¹⁰ found atomic-scale defects similar to that proposed by Pandey by scanning tunneling microscopy (STM). The missing dimer occurred rather often but at random. They reported the density of the defects depends on the sample preparation. We discuss here the ordering of the missing-dimer defects in terms of the lattice distortion caused by the defects and propose that one of the possible arrangements of the defects corresponds to the (2×8) reconstruction observed by LEED.

First of all, we assume that the electronic energy lowering by a single-defect formation surpasses the strain energy increase. We should then mainly consider the interaction energy between defects. Figure 2(a) illustrates the Si(001) surface with a single missing-dimer defect and Figs. 2(b) and 2(c) with pairs of defects of type I and type II, respectively. The arrows in Fig. 2(a) schematically indicate the distortion field caused by the defect. It is clear that this distortion field makes the type-I pair less stable than the type-II pair, in other words, the repulsion in the type-I defect pair is stronger. Supported by these arguments and for the sake of simplicity, we now restrict ourselves to consider only the case where defects occur side by side along the direction perpendicular to the rows of dimers. This corresponds to a (2× n) periodicity, which is schematically represented in Fig. 3.

With a given atomic arrangement of the (2× n) periodicity, we have carried out the minimization of the surface strain energy. To illustrate the strain distortion field clearly, we define the repulsion energy between defects, $\epsilon_{\text{rep, AS}}$

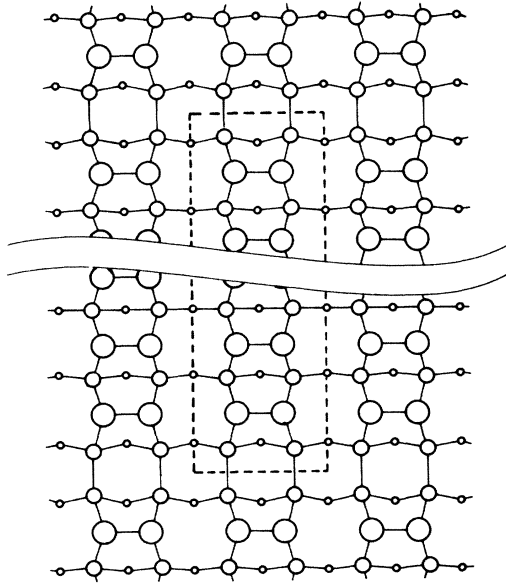


FIG. 3. Ordered-defect model for the Si(001)-(2×*n*) surface.

$$E_s^{2 \times n} = (n - 1)\epsilon_{\text{dim}} + \epsilon_{\text{def}} + \epsilon_{\text{rep}},$$

where $E_s^{2 \times n}$ is the total elastic strain energy of the (2×*n*) unit mesh, ϵ_{dim} and ϵ_{def} are the elastic strain energies due to a single dimer and a single defect, respectively. ϵ_{dim} is calculated as the strain energy of the (2×1) structure with no defect. ϵ_{def} was determined from that of the (2×20) structure, which may be large enough to ignore the interaction between the defects.

In order to estimate the elastic strain energy E_s , we employ a Keating's model,¹¹ in which the elastic energy due to atomic displacements is expressed as

$$E_s = \alpha \sum_{\text{all bonds}} (|\mathbf{X}_{ij}|^2 - X_0^2)^2 + \beta \sum_{\text{all bond pairs}} (\mathbf{X}_{ij} \cdot \mathbf{X}_{jk} - X_0^2 \cos \theta)^2,$$

where \mathbf{X}_{ij} is a relative atomic displacement vector, and X_0 and θ are the equilibrium bond length and bond angle, respectively. Here X_0 was fixed to the bulk value, 2.35 Å, and θ to 109.47°. Atoms to the eighth layer were allowed to displace from the bulk positions. If the electron configuration of the topmost-layer atoms are assumed to be sp^2 , X_0 must be shortened to some extent for a dimer bond and θ must be fixed to 120° for bond pairs including a dimer bond. This modification was actually done but did not have an affect on the final conclusion. In the calculation, the ratio β/α was fixed to that of bulk Si, 0.29, where α and β denote force constants of bond stretching and bond bending, respectively. Figure 4 shows the calculated values of ϵ_{rep} as a function of *n*. Although the determination of *n* corresponding to the most stable structure requires careful consideration about the electronic energy, it can at least be said that the distortion is not so severe for the structure of *n* = 8, which is thought to correspond to the observed (2×8) structure.

It is evident that the ordered-defect model fulfills the

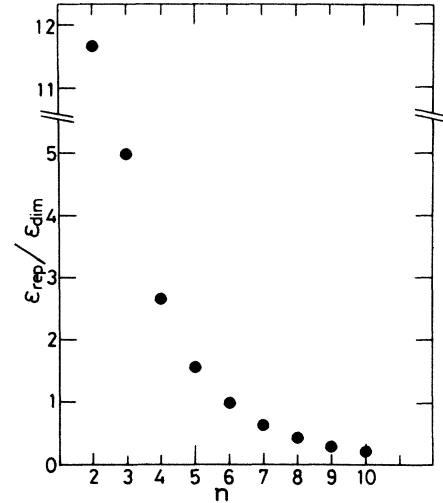


FIG. 4. Repulsion energy between defects ϵ_{rep} as a function of *n*.

criteria deduced from the observed LEED patterns. First, the basic atomic arrangement in this model is essentially the same as that of the (2×1) structure, except that every eighth dimer is absent. Secondly, the elastic strain due to the defects causes the lateral expansion of the surface layers. For the (2×8) ordered-defect structure, atomic positions of which have been adjusted to minimize the surface strain energy, spacings between adjacent dimers are expanded by 4.5–8.6%. These features are in good agreement with the LEED results mentioned before. We now calculate kinematical LEED intensity from the (2×8) structure. Figure 5 represents the calculated LEED pattern for the optimized ordered-defect model. The intensity of each eighth-order spot was averaged over incident electron energy of 30–140 eV. The pronounced features observed in the (2×8) surface are well reproduced. The

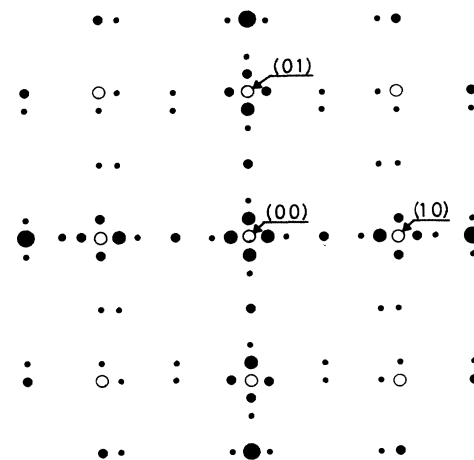


FIG. 5. Kinematically calculated LEED pattern for the Si(001)-(2×8) ordered-defect structure. The radius of circles is proportional to the intensity of each eighth-order spot.

strong similarity between observed and calculated LEED patterns provide here a support for the ordered-defect model for the Si(001)-(2×8) structure.

Finally we discuss the mechanism of the formation of the (2×8) structure. One possible elucidation of the phenomenon is that the (2×1) structure is more stable than the (2×8) structure in the ideal situation but some factors, e.g., lattice distortion and electronic rehybridization due to Ni impurity, macroscopic strain due to the less ideal sample holding, lower the total energy of the (2×8) structure. It is well known that the the deposition of Ni on Si surfaces followed by annealing results in the epitaxial growth of NiSi₂ layers. The slight difference of the lattice constants between Si (5.431 Å) and NiSi₂ (5.406 Å) might be large enough to cause the lattice distortion and change the surface structure.

Another elucidation argues that, even in the clean surface, the missing-dimer defect structure is indeed more stable than the (2×1) structure but cannot be ordered by usual preparation conditions. This situation is possible, for example, as follows: The ordering of the missing-

dimer defects may accompany a high activation energy, since the ordering of the defects requires the transfer of surface silicon atoms. Then the ordering of defects into the (2×8) periodicity requires annealing at high temperatures. On the other hand, the evaporation of surface silicon atoms from step sites is also enhanced at high temperatures. If the evaporation rate or the progression rate of the steps is faster than the ordering rate, the (2×8) structure cannot be formed even though it is the most stable structure. The realization of the (2×8) structure is then achieved by the suppression of the evaporation, which may be caused by the step pinning due to segregation of Ni atoms on surface steps. At any rate, these mechanisms are possible but without experimental supports at this time. Further studies are required to reveal the formation mechanism of the (2×8) structure and the relevance of the model to other structures observed on the Si(001) surface.⁶

We are grateful to Dr. H. Tochiyama and Dr. T. Tabata for helpful discussions.

*Present address: Department of Chemistry, Faculty of Science, The University of Tokyo, Hongo, Bunkyo-ku, Tokyo 113, Japan.

¹D. J. Chadi, *Phys. Rev. Lett.* **43**, 43 (1979).

²M. T. Yin and M. L. Cohen, *Phys. Rev. B* **24**, 2303 (1981).

³T. Tabata, T. Aruga, and Y. Murata, *Surf. Sci.* (to be published).

⁴J. Ihm, D. H. Lee, J. D. Joannopoulos, and J. J. Xiong, *Phys. Rev. Lett.* **51**, 1872 (1983).

⁵A. Saxena, E. T. Gaulinski, and J. D. Gunton, *Surf. Sci.* **160**, 618 (1985).

⁶K. Muller, E. Lang, L. Hammer, W. Grim, P. Heilman, and K. Heinz, in *Determination of Surface Structure by LEED*, edited

by P. M. Marcus and F. Jona (Plenum, New York, 1984), p. 483.

⁷E. G. McRae, R. A. Malic, and D. A. Kapilow, *Rev. Sci. Instrum.* **56**, 2077 (1985).

⁸K. Kato, T. Ide, S. Miura, and T. Ichinokawa (unpublished).

⁹K. C. Pandey, in *Proceedings of the Seventeenth International Conference on the Physics of Semiconductors*, edited by D. J. Chadi and W. A. Harrison (Springer-Verlag, New York, 1985), p. 55.

¹⁰R. M. Tromp, R. J. Hamers, and J. E. Demuth, *Phys. Rev. Lett.* **55**, 1303 (1985).

¹¹P. N. Keating, *Phys. Rev.* **145**, 637 (1966).

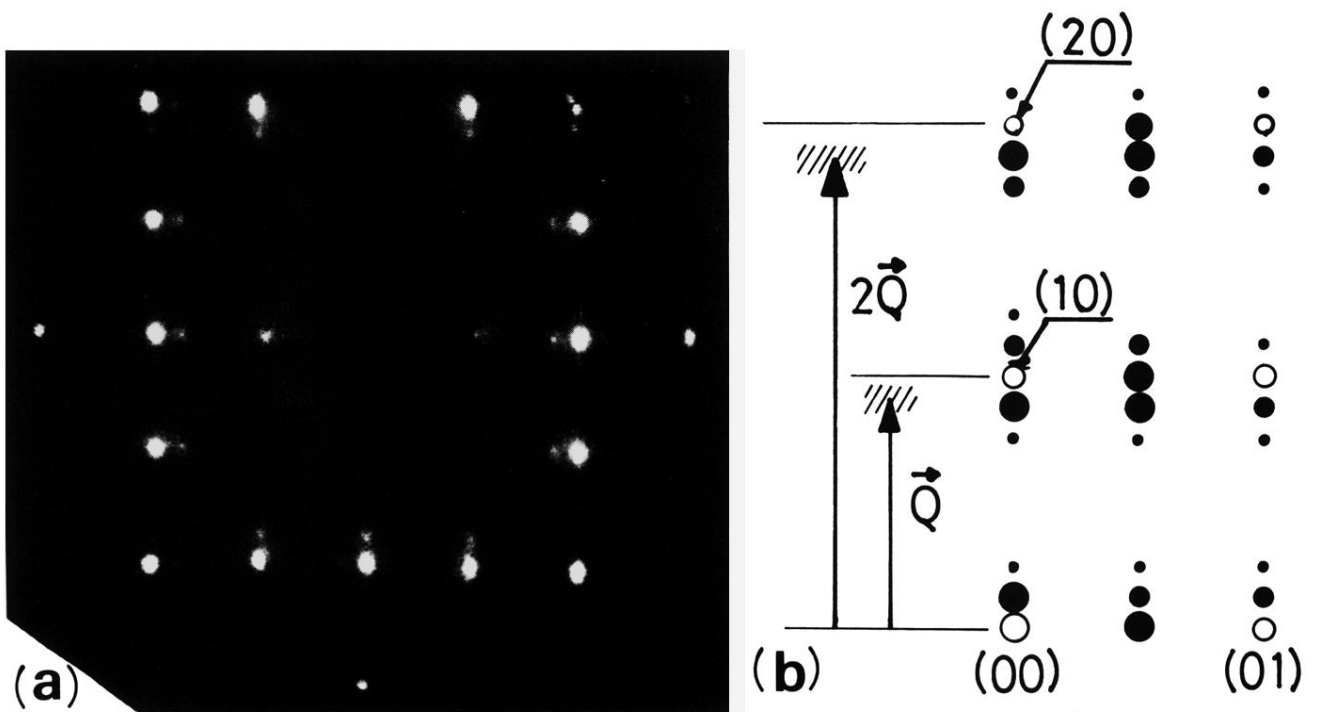


FIG. 1. (a) Typical LEED pattern of normal incidence from the two-domain Si(001)-(2 \times 8) surface. Primary electron energy is 47 eV. (b) Averaged LEED pattern. Only the contribution from one of the two orthogonal domains is shown for the sake of simplicity.